www.elsevier.nl/locate/jorganchem

Journal of Organometallic Chemistry 614–615 (2000) 153–157

Closo and semipseudocloso forms of the same carbametallaborane: synthesis and spectroscopic and crystallographic characterisation of 1-CCPh-2-Ph-3-(η-L)-3,1,2-$RhC_2B_9H_9$ (L = C_5H_5 and C_5Me_5)☆

Part 25. Steric effects in heteroboranes

Rhona M. Garrioch, Georgina M. Rosair, Alan J. Welch *

Department of Chemistry, Heriot-Watt University, Edinburgh, EH14 4AS, UK

Received 3 April 2000

Dedicated to Prof. Sheldon Shore on the occasion of his 70th birthday in recognition of his many outstanding contributions to polyhedral boron chemistry.

Abstract

The compounds of 1-CCPh-2-Ph-3-(η-L)-3,1,2-$RhC_2B_9H_9$ (L = C_5H_5, **1**, and C_5Me_5, **2**) have been prepared. The weighted average ^{11}B-NMR chemical shift ($\langle\delta\,^{11}B\rangle$) for **1** is + 2.53 ppm, suggesting that the cage is distorted into a semipseudocloso structure. For **2** in $CDCl_3$ $\langle\delta\,^{11}B\rangle$ is − 0.7 ppm, between that anticipated for semipseudocloso and closo forms. Compound **2** crystallises in two different forms. Orange **2a** is semipseudocloso, with C(1)–C(2) 2.052(5) Å, whilst yellow **2b** is essentially closo, with C(1)–C(2) 1.828(7) Å. Dissolution of both **2a** and **2b** in $CDCl_3$ affords an identical solution. © 2000 Elsevier Science B.V. All rights reserved.

Keywords: Closo; Semipseudocloso; Carbametallaborane; Crystallographic characterisation; Pseudocloso

1. Introduction

In recent publications we have shown how preorganising for carbametallaboranes to be sterically overcrowded can lead to interesting and unusual structures [1]. The Ph substituents in [7,8-Ph_2-7,8-*nido*-$C_2B_9H_{10}$]$^-$ [2] (and, presumably, its deprotonated analogue) stand approximately perpendicular to the C_2B_3 open face, a conformation described by θ values near zero (θ is the modulus of the average C_{cage}–C_{cage}–C_{ipso}–C_{phenyl} torsion angle [3]). When, however, [7,8-Ph_2-7,8-*nido*-$C_2B_9H_9$]$^{2-}$ is metallated with a {Cp*Rh}$^{2+}$ (Cp* = η-C_5Me_5) [4] or {(arene) Ru}$^{2+}$ [5] fragment the Ph substituents twist to high θ values and push against each other. This results in a prising open of the C(1)–C(2) connectivity from ca. 1.7 to ca. 2.5 Å and a concomitant contraction of the M(3)···B(6) distance from ca. 3.5 to ca. 3.0 Å, thus producing a nearly square MCBC face in the distorted cluster. Such distorted cages are termed ‘pseudocloso’[1] and appear geometrically to lie between 12-vertex closo and hypercloso forms (Fig. 1). Spectroscopically pseudocloso carbametallaboranes are characterised by ^{11}B-NMR resonances which lie to high frequency of those of closo analogues, with $\langle\delta\,^{11}B\rangle$ ca. + 6 ppm (pseudocloso) cf. $\langle\delta\,^{11}B\rangle$ ca. − 9 ppm (closo).

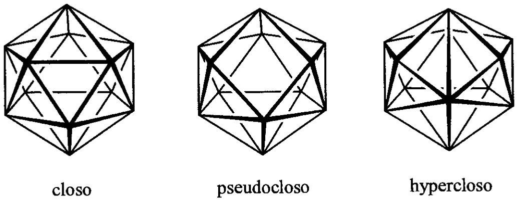

Fig. 1. Closo, pseudocloso and hypercloso 12-vertex polyhedra.

☆ For Part 24, see Acta Crystallogr. Sect. C 56 (2000) 487.

* Corresponding author. Tel.: + 44-131-4513217; fax: + 44-131-4513180.

E-mail address: a.j.welch@hw.ac.uk (A.J. Welch).

[1] Very recently a pseudocloso carbametallaborane with Ph and SPh substituents attached to the cage carbon atoms has been reported (see [6]).

PII: S0022-328X(00)00572-6

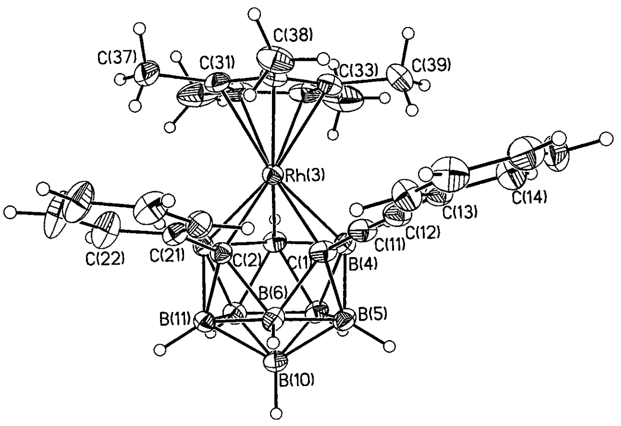

Fig. 2. Perspective view of a single molecule of compound **2a**. Thermal ellipsoids are drawn at 50% probability level, except for H atoms. Phenyl rings numbered cyclically.

We have also shown that using C_{cage} substituents which are slightly less sterically demanding than Ph can lead to only partially deformed carbametallaboranes. Thus, 1-CCPh-2-Ph-3-(η-cymene)-3,1,2-$RuC_2B_9H_9$ [7] (cymene = $C_6H_4Me^iPr$-1,4) displays a 'semipseudocloso' structure with C(1)···C(2) 2.184 Å, Ru(3)···B(6) 3.166 Å, and $\langle\delta^{11}B\rangle$ + 2.4 ppm. The isolation of pseudocloso and semipseudocloso compounds implies a continuum of structure type from closo to hypercloso, and since the former is characterised by $(n+1)$ [8] and the latter by only n [9] skeletal electron pairs it is clearly interesting to speculate on the most appropriate (electronic) description of intermediate shapes.

In this paper we report two further examples of such intermediate, partially distorted, carbametallaboranes. Solution studies suggest that one is semipseudocloso in shape, whilst the other is intermediate between closo and semipseudocloso. Intriguingly, this latter species crystallises in two forms, one closo and the other semipseudocloso.

2. Results and discussion

The reaction between Tl_2[7-CCPh-8-Ph-7,8-*nido*-$C_2B_9H_9$], in slight excess, and $[CpRhCl_2]_n$ in CH_2Cl_2 leads to a modest yield of the yellow–brown solid **1** after chromatographic work-up. Although single crystals of **1** could not be obtained in spite of numerous attempts the compound is confidently formulated as semipseudocloso 1-CCPh-2-Ph-3-(η-C_5H_5)-3,1,2-$RhC_2B_9H_9$ on the basis of elemental analysis and ^{11}B- and ^1H-NMR spectroscopy.

The ^1H-NMR spectrum of **1** is as expected, with multiplet resonances in the aromatic region (C_6H_5, 10H) and a singlet at 5.45 ppm (C_5H_5, 5H). The $^{11}B-\{^1H\}$-NMR spectrum reveals six peaks of relative integral 1:1:2:2:2:1 (high frequency to low frequency) at 128.4 MHz. That the integral-2 resonances are co-incidences is supported by the higher frequency pair being significantly broader at half-height than the integral-1 resonances. Each resonance appears as a doublet (J_{BH} = 120–155 Hz) in the ^{11}B spectrum. Importantly, the weighted average ^{11}B chemical shift ($\langle\delta^{11}B\rangle$) for **1** is + 2.5 ppm, giving a clue to the nature of the cage.

Previous studies on the pseudocloso carbametallaboranes 1,2-Ph_2-3-(η-L)-3,1,2-$MC_2B_9H_9$ for LM = Cp*Rh [4], (C_9Me_7)Rh [10], (C_6H_6)Ru [5], (cymene)Ru [5], and (C_6Me_6)Ru [5] (with the structures of the first four of these confirmed by crystallographic studies) have revealed $\langle\delta^{11}B\rangle$ values in the narrow range + 5.4 to + 6.4 ppm, i.e. effectively independent of whether the metal fragment is (η^5-C_5)Rh or (η^6-C_6)Ru. Thus, given that the compound 1-CCPh-2-Ph-3-(η-cymene)-3,1,2-$RuC_2B_9H_9$ [7] has a $\langle\delta^{11}B\rangle$ value of + 2.4 ppm and a structure shown to be semipseudocloso in type [C(1)···C(2) 2.18 Å] we can be confident that a very similar structure is possessed by **1**.

Reaction of Tl_2[7-CCPh-8-Ph-7,8-*nido*-$C_2B_9H_9$] with $[Cp^*RhCl_2]_2$ in CH_2Cl_2 (again with the carbaborane in slight excess) leads to the formation of 1-CCPh-2-Ph-3-(η-C_5Me_5)-3,1,2-$RhC_2B_9H_9$, **2**, the Cp* analogue of compound **1**. The yield of compound **2** is significantly better than that achieved for **1**, presumably a consequence of the fact that $[Cp^*RhCl_2]_2$ is soluble in CH_2Cl_2 whilst $[CpRhCl_2]_n$ is not.

In $CDCl_3$ compound **2** is yellow. The ^1H-NMR spectrum reveals resonances assigned to aromatic and to methyl protons in the correct relative ratio (2:3). In the $^{11}B-\{^1H\}$-NMR spectrum are eight resonances (1:1:1:1:2:1:1:1, high to low frequency) all of which are doublets (J_{BH} = 130–160 Hz) in the proton-coupled spectrum. The $\langle\delta^{11}B\rangle$ value for **2** is − 0.7 ppm. Correlating this with the degree of distortion of the cluster suggests a structure between closo ($\langle\delta^{11}B\rangle$ ca. − 9 ppm) and semipseudocloso ($\langle\delta^{11}B\rangle$ ca. + 2.5 ppm), i.e. showing less distortion than that observed in compound **1**.

Intriguingly, slow evaporation of a (yellow) CH_2Cl_2 solution of **2** yields both orange blocks (**2a**) and pale yellow plates (**2b**), each as diffraction-quality single crystals.

A perspective view of **2a** is shown in Fig. 2 and Table 1 lists selected interatomic distances and interbond angles. The structure of **2a** is semipseudocloso, C(1)···C(2) = 2.052(5) Å, Rh(3)···B(6) = 3.230(4) Å. The θ values of the Ph and CCPh rings are similar to each other, 80.8° and 71.8° respectively, and Ph···CCPh contacts < 3 Å are H(26)···C(11) (2.62 Å), H(26)···H(18) (2.89 Å) and H(26)···C(12) (2.89 Å).

A single molecule of **2b** is shown in Fig. 3, with Table 2 showing the key molecular parameters derived. It is immediately apparent that the best description of **2b** is that of a closo carbametallaborane with a formal C(1)–

C(2) connectivity, although at 1.828(7) Å this is somewhat longer than normal.[2] The Rh(3)···B(6) distance, 3.375(5) Å, is significantly longer than that in **2a**. These distances for both **2a** and **2b** are summarised in Fig. 4, together with the internal angles in the RhCCB fragments. Clearly the Rh(3)C(1)B(6)C(2) unit in **2b** is best described as a diamond, with that of **2a** being distinctly distorted towards a square. In **2b** the Ph ring on C(2) has a broadly similar conformation with respect to the cluster as that in **2a** ($\theta = 72.0°$) but the CCPh unit is significantly twisted, to $\theta = 29.3°$. Ph···CCPh contacts

Table 1
Selected interatomic distances (Å) and interbond angles (°) for **2a**

Rh(3)–C(1)	2.136(4)	Rh(3)–C(2)	2.168(3)
Rh(3)–B(4)	2.179(4)	Rh(3)–B(7)	2.190(4)
Rh(3)–B(8)	2.198(4)	Rh(3)–C(31)	2.232(3)
Rh(3)–C(32)	2.252(3)	Rh(3)–C(33)	2.210(3)
Rh(3)–C(34)	2.173(4)	Rh(3)–C(35)	2.190(4)
C(1)–C(2)	2.052(5)	C(1)–C(11)	1.439(5)
C(1)–B(4)	1.691(5)	C(1)–B(5)	1.662(5)
C(1)–B(6)	1.718(5)	C(2)–B(6)	1.726(5)
C(2)–B(7)	1.687(5)	C(2)–B(11)	1.662(5)
C(2)–C(21)	1.506(4)	B(4)–B(5)	1.795(6)
B(4)–B(8)	1.828(6)	B(4)–B(9)	1.788(5)
B(5)–B(6)	1.784(6)	B(5)–B(9)	1.764(6)
B(5)–B(10)	1.756(6)	B(6)–B(10)	1.802(5)
B(6)–B(11)	1.777(6)	B(7)–B(8)	1.839(6)
B(7)–B(11)	1.800(6)	B(7)–B(12)	1.800(5)
B(8)–B(9)	1.787(6)	B(8)–B(12)	1.795(6)
B(9)–B(10)	1.779(6)	B(9)–B(12)	1.769(6)
B(10)–B(11)	1.757(6)	B(10)–B(12)	1.774(6)
B(11)–B(12)	1.771(6)	C(11)–C(12)	1.181(5)
C(12)–C(13)	1.446(5)		
C(1)–Rh(3)–C(2)	56.94(14)	C(11)–C(1)–Rh(3)	113.4(2)
C(11)–C(1)–C(2)	113.44(3)	C(11)–C(1)–B(4)	125.8(3)
C(11)–C(1)–B(5)	117.9(3)	C(11)–C(1)–B(6)	113.5(3)
C(21)–C(2)–Rh(3)	116.0(2)	C(21)–C(2)–C(1)	118.41(3)
C(21)–C(2)–B(7)	125.7(3)	C(21)–C(2)–B(6)	114.0(3)
C(21)–C(2)–B(11)	116.6(3)	B(6)–C(1)–Rh(3)	113.5(2)
B(6)–C(2)–Rh(3)	111.6(2)	C(1)–B(6)–C(2)	73.1(2)

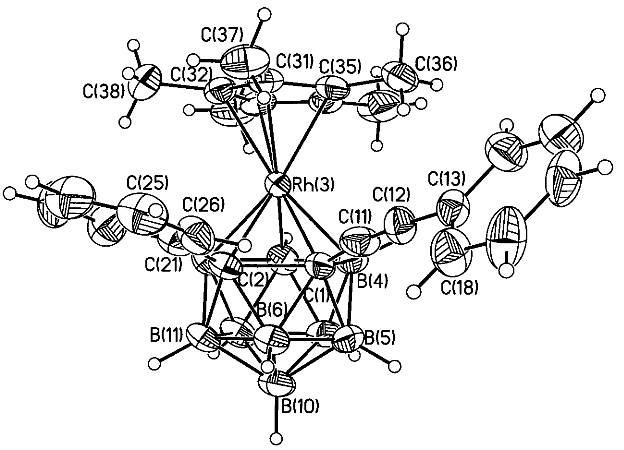

Fig. 3. Perspective view of a single molecule of compound **2b**, drawn as for Fig. 1.

Table 2
Selected interatomic distances (Å) and interbond angles (°) for **2b**

Rh(3)–C(1)	2.161(4)	Rh(3)–C(2)	2.179(5)
Rh(3)–B(4)	2.186(5)	Rh(3)–B(7)	2.176(5)
Rh(3)–B(8)	2.187(6)	Rh(3)–C(31)	2.247(5)
Rh(3)–C(32)	2.209(5)	Rh(3)–C(33)	2.169(4)
Rh(3)–C(34)	2.185(4)	Rh(3)–C(35)	2.230(4)
C(1)–C(2)	1.828(7)	C(1)–B(4)	1.722(7)
C(1)–B(5)	1.692(7)	C(1)–B(6)	1.723(6)
C(1)–C(11)	1.440(7)	C(2)–B(6)	1.728(7)
C(2)–B(7)	1.730(7)	C(2)–B(11)	1.672(6)
C(2)–C(21)	1.516(6)	B(4)–B(5)	1.791(7)
B(4)–B(8)	1.818(8)	B(4)–B(9)	1.790(8)
B(5)–B(10)	1.762(8)	B(5)–B(6)	1.767(8)
B(5)–B(9)	1.774(9)	B(6)–B(10)	1.790(8)
B(6)–B(11)	1.767(8)	B(7)–B(11)	1.797(7)
B(7)–B(12)	1.775(8)	B(7)–B(8)	1.815(8)
B(8)–B(9)	1.800(8)	B(8)–B(12)	1.782(7)
B(9)–B(10)	1.786(8)	B(9)–B(12)	1.797(9)
B(10)–B(11)	1.772(9)	B(10)–B(12)	1.786(9)
B(11)–B(12)	1.771(9)	C(11)–C(12)	1.184(7)
C(12)–C(13)	1.453(6)		
C(1)–Rh(3)–C(2)	49.80(18)	C(11)–C(1)–Rh(3)	112.8(3)
C(11)–C(1)–C(2)	123.3(4)	C(11)–C(1)–B(4)	121.8(4)
C(11)–C(1)–B(5)	115.0(4)	C(11)–C(1)–B(6)	113.6(4)
C(21)–C(2)–Rh(3)	113.6(3)	C(21)–C(2)–C(1)	122.6(4)
C(21)–C(2)–B(6)	112.9(4)	C(21)–C(2)–B(7)	123.9(5)
C(21)–C(2)–B(11)	115.8(4)	B(6)–C(1)–Rh(3)	120.3(3)
B(6)–C(1)–C(2)	58.2(3)	B(6)–C(2)–Rh(3)	119.0(3)
C(1)–B(6)–C(2)	64.0(3)		

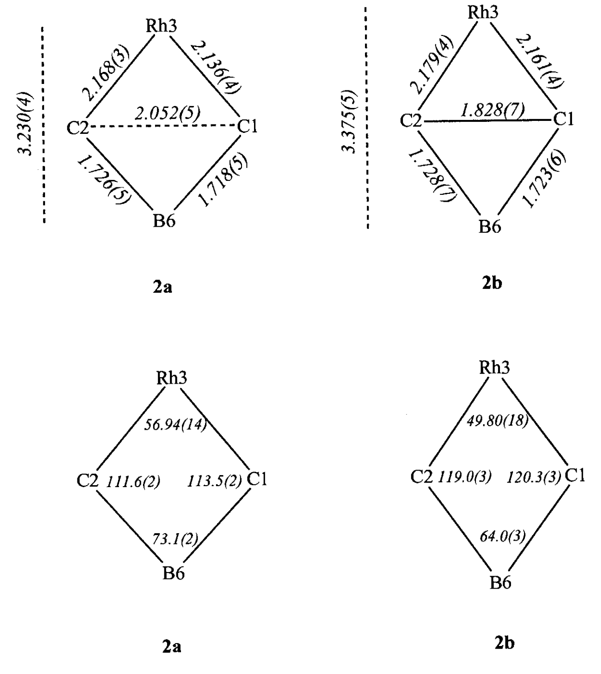

Fig. 4. Key molecular parameters in the Rh(3)C(1)B(6)C(2) fragments of compounds **2a** and **2b**.

---

[2] For example, in 3-(η-C_5H_5)-3,1,2-$CoC_2B_9H_{11}$ the C(1)–C(2) distance is 1.637(6) Å (see [11]).

< 3 Å in **2b** are H(26)···C(11), 2.54 Å and H(26)···C(12), 2.88 Å. Presumably the origin of the reduced θ value of the CCPh unit in **2b** is the avoidance of an unacceptably short H(26)···H(18) contact.

Dissolution of both **2a** and **2b** in $CDCl_3$ affords (yellow) solutions which are spectroscopically identical ($\langle\delta^{11}B\rangle = -0.7$ ppm). Clearly the closo–semipseudocloso transformation is relatively facile and it may be that this is related to the apparent ability of subtle changes in the molecule to affect the structure. Thus, the replacement of Cp in **1** by Cp* in **2** (with greater inductive effect) is able to moderate the closo → semipseudocloso distortion (this distortion is associated with a reduction in the formal cluster electron count). In contrast it seems that pseudocloso structures are less susceptible to such changes, since the geometry of 1,2-Ph_2-3-(η-L)-3,1,2-$RuC_2B_9H_9$ is essentially invariant along the series L = (C_6H_6), (cymene), (C_6Me_6) [5].

3. Experimental

3.1. Synthetic and spectroscopic

Experiments were performed under dry, oxygen-free N_2 using standard Schlenk techniques, with some subsequent manipulation in the open laboratory. Solvents were freshly distilled over CaH_2 (CH_2Cl_2) or Na wire (THF, 60–80 petroleum ether) or stored over 4 Å molecular sieves (MeOH). Preparative thin layer chromatography (TLC) employed 20 × 20 cm Kieselgel 60 F_{254} glass plates. NMR spectra at 400.1 MHz (^1H), or 128.4 MHz (^{11}B) were recorded on a Bruker DPX 400 spectrometer as $CDCl_3$ solutions at ambient temperature. Elemental analyses were determined by the departmental service. The starting materials Tl_2[7-CCPh-8-Ph-7,8-*nido*-$C_2B_9H_9$] [6], $[CpRhCl_2]_n$ [12] and $[Cp^*RhCl_2]_2$ [13] were prepared by literature methods or slight variants thereof.

3.2. Synthesis of *1*

To a frozen (−196°C) suspension of Tl_2[7-CCPh-8-Ph-7,8-*nido*-$C_2B_9H_9$] (0.104 g, 0.15 mmol) in CH_2Cl_2 (5 cm^3), in a foil covered Schlenk tube, was added a suspension of $[CpRhCl_2]_n$ (0.027 g, 0.11 mmol Rh) in the same solvent (5 cm^3) and the components re-frozen. The reaction mixture was then allowed to warm slowly to room temperature (r.t.) and stirred overnight. The solid formed was removed by Schlenk filtration through Celite® and the brown filtrate reduced in volume in vacuo. Purification by preparative TLC (4:1, CH_2Cl_2/60–80 petroleum ether) gave a yellow–brown mobile band (R_f 0.9) yielding a brown solid. Attempted crystallisations from a variety of solvents did not afford diffraction-quality crystals.

3.2.1. Compound *1*

1-CCPh-2-Ph-3-(η-C_5H_5)-3,1,2-$RhC_2B_9H_9$, yield = 0.011 g (20%). $C_{21}H_{24}B_9Rh$ requires: C 52.9; H, 5.00. Found: C, 53.6; H, 5.94%. $^{11}B-\{^1H\}$-NMR: δ 21.39 (1B), 12.73 (1B), 3.06 (2B), 0.48 (2B), −1.27 (2B), and −15.87 (1B) ppm; ^1H-NMR: δ 7.81–7.74 (m, 2H, C_6H_5), 7.51–7.18 (m, 8H, C_6H_5) and 5.45 (s, 5H, C_5H_5) ppm.

3.3. Synthesis of *2*

Similarly, Tl_2[7-CCPh-8-Ph-7,8-*nido*-$C_2B_9H_9$] (0.264 g, 0.37 mmol) in CH_2Cl_2 (5 cm^3) was reacted with of $[Cp^*RhCl_2]_2$ (0.106 g, 0.34 mmol Rh) in the same solvent (10 cm^3). Work-up as previously yielded a red–brown solution affording a single yellow mobile band on TLC (R_f 0.85) from which was obtained a yellow solid.

3.3.1. Compound *2*

1-CCPh-2-Ph-3-(η-C_5Me_5)-3,1,2-$RhC_2B_9H_9$, yield = 0.092 g (49%). $C_{26}H_{34}B_9Rh$ requires: C, 57.1; H, 6.27. Found: C, 56.8; H, 6.16%. $^{11}B-\{^1H\}$-NMR: δ 17.99 (1B), 6.32 (1B), 3.39 (1B), 1.01 (1B), −4.68 (2B), −5.82 (1B), −6.65 (1B) and −13.48 (1B) ppm; ^1H-NMR: δ 7.62–7.57 (m, 2H, C_6H_5), 7.50–7.46 (m, 2H, C_6H_5), 7.40–7.38 (m, 2H, C_6H_5), 7.28–7.24 (m, 2H, C_6H_5), 7.18–7.13 (m, 2H, C_6H_5) and 1.61 (s, 15H, $C_5(CH_3)_5$) ppm. Slow evaporation of a CH_2Cl_2 solution of compound **2** yielded approximately equal amounts of two crystalline forms, orange **2a** and yellow **2b**, separated by hand. Solutions of **2a** and of **2b** in $CDCl_3$ are both yellow. They were examined by IR and ^{11}B-NMR spectroscopies and found to be identical (IR: ν_{max} at 2542 cm^{-1}; NMR as above).

3.4. Crystallography

Single crystals of **2a** and **2b** were mounted in subsequently sealed thin-walled glass capillaries with epoxy resin glue. Intensity measurements were carried out at r.t. on a Siemens P4 Diffractometer [14] with graphite-monochromated Mo–K_α radiation ($\lambda = 0.71069$ Å) using ω-scans. Table 3 lists details of unit cell data, intensity data collection and structure refinement. Standard reflections were re-measured every 100 data and crystal decay corrected. Data were corrected for absorption by ψ-scans. Both structures were solved by direct and difference Fourier methods and refined [15] by full-matrix least-squares against F^2, with non-hydrogen atoms assigned anisotropic displacement parameters. Phenyl and methyl H atom positions were calculated and treated as riding models with displacement parameters calculated as 1.2 or 1.5 times the bound carbon atom U_{eq}, respectively.

Table 3
Crystallographic data for compounds **2a** and **2b** [a]

	2a	**2b**
Crystal colour and habit	Orange block	Pale yellow plate
Crystal size (mm)	$0.16 \times 0.29 \times 0.22$	$0.88 \times 0.47 \times 0.08$
Formula	$C_{26}H_{34}B_9Rh$	$C_{26}H_{34}B_9Rh$
M	546.73	546.73
System	Monoclinic	Monoclinic
Space group	$P2_1/c$	$P2_1/c$
Unit cell dimensions		
a (Å)	11.7641(6)	13.5958(16)
b (Å)	12.3997(6)	12.3617(15)
c (Å)	18.6998(11)	17.3815(18)
β (°)	99.643(5)	112.003(8)
U (Å^3)	2689.2(3)	2708.5(5)
Z	4	4
D_{calc}	1.350	1.341
μ(Mo–K$_\alpha$) (mm^{-1})	0.650	0.645
$\theta_{\text{data collection}}$ (°)	1.76–25.00	2.08–25.00
Data measured, % decay	6033, 8.95	5926, 3.12
Unique data, R_{int}	4740, 0.0235	4739, 0.0289
Observed data [$I > 2\sigma(I)$]	3771	3595
R, wR_2, S (all data)	0.0525, 0.0807, 1.023	0.0634, 0.1030, 1.056
Variables	325	325
$E_{\max}$, $E_{\min}$ (e Å^{-3}))	0.320, −0.315	0.385, −0.328

[a] $R = \Sigma||F_o|-|F_c|/\Sigma|F_o|$, $wR_2 = [\Sigma[w(F_o^2 - F_c^2)^2]/\Sigma w(F_o^2)^2]^{0.5}$ (where $w^{-1} = [\sigma_c^2(F_o)^2 + (aP)^2 + bP]$ and $P = [0.333\max\{F_o, 0\} + 0.667(F_o)^2]$), $S = [\Sigma[w(F_o^2 - F_c^2)^2/(n-p)]^{0.5}$ (where n is the number of data and p the number of parameters).

4. Supplementary material

Crystallographic data for the structures reported in this paper have been deposited with the Cambridge Crystallographic Data Centre, CCDC no. 145236 for compound **2a** and CCDC no. 145237 for compound **2b**. Copies of this information may be obtained free of charge from the Director, CCDC, 12 Union Road, Cambridge, CB2 1EZ, UK (fax: +44-1223-336-033; e-mail: deposit@ccdc.cam.ac.uk or http://www.ccdc.cam.ac.uk).

Acknowledgements

We thank the EPSRC for support (RMG), Mr. G. Evans for microanalysis and Dr. A.S.F. Boyd for NMR spectra.

References

[1] A.J. Welch, in: P. Braunstein, L.A. Oro, P.R. Raithby (Eds.), Steric Effects in Metallacarboranes in Metal Clusters in Chemistry, Wiley-VCH, 1999, p. 26.
[2] J. Cowie, D.J. Donohoe, N.L. Douek, A.J. Welch, Acta Crystallogr. Sect. C 49 (1993) 710.
[3] J. Cowie, B.D. Reid, J.M.S. Watmough, A.J. Welch, J. Organomet. Chem. 481 (1994) 283.
[4] Z.G. Lewis, A.J. Welch, J. Organomet. Chem. 430 (1992) C45.
[5] P.T. Brain, M. Bühl, J. Cowie, Z.G. Lewis, A.J. Welch, J. Chem. Soc. Dalton Trans. (1996) 231.
[6] F. Teixidor, M.A. Flores, C. Viñas, R. Sillanpää, R. Kivekäs, J. Am. Chem. Soc. 122 (2157) 1963.
[7] Rh. Ll. Thomas, A.J. Welch, J. Chem. Soc. Dalton Trans. (1997) 631.
[8] (a) K. Wade, J. Chem. Soc. Chem. Commun. (1976) 792. (b) K. Wade, Adv. Inorg. Chem. Radiochem. 18 (1976) 1.
[9] (a) R.T. Baker, Inorg. Chem. 25 (1986) 109. (b) R.L. Johnston, D.M.P. Mingos, Inorg. Chem. 25 (1986) 3321.
[10] U. Grädler, A.S. Weller, A.J. Welch, D. Reed, J. Chem. Soc. Dalton Trans. (1996) 335.
[11] D.E. Smith, A.J. Welch, Organometallics 5 (1986) 760.
[12] J.W. Kang, K. Mosely, P.M. Maitlis, J. Am. Chem. Soc. 91 (1969) 5970.
[13] C. White, A. Yates, P.M. Maitlis, Inorg. Synth. 29 (1992) 228.
[14] Siemens Analytical Instruments, Inc., Madison, WI, USA, 1996.
[15] G.M. Sheldrick, SHELXTL Version 5.1, Bruker AXS Inc, Madison, WI, USA, 1999.